Natural Hydrophobicity and Reversible Wettability Conversion of Flat Anatase TiO₂ Thin Film

Jian-Yun Zheng,[†,‡] Shan-Hu Bao,[†] Yu Guo,[†,‡] and Ping Jin*,[†,§]

[†]State Key Laboratory of High Performance Ceramics and Superfine Microstructure, Shanghai Institute of Ceramics, Chinese Academy of Sciences, Shanghai 200050, China

[‡]Graduate School of Chinese Academy of Sciences, Beijing 100049, China

[§]National Institute of Advanced Industrial Science and Technology (AIST), Moriyama, Nagoya 463-8560, Japan

Ⓢ *Supporting Information*

ABSTRACT: Flat anatase TiO₂ thin film deposited at room temperature shows the natural hydrophobicity, which is destroyed by 400 °C vacuum annealing. On the basis of the analysis of surface composition and structure, the origin of hydrophobicity of the flat TiO₂ film can be identified as (1) approximately fully stoichiometric TiO₂ and (2) hydrocarbon adsorbates on the film surface. We further validate that interfacial water molecules near the surface of the as-prepared TiO₂ film are oriented in the hydrophobic hydration structure via Fourier transform infrared/attenuated total reflection. Moreover, the as-prepared TiO₂ film also shows a smart surface reversibly switched between hydrophobicity and super-hydrophilicity. During the recovery process of hydrophobicity, the irradiated films show the wettability with water contact angle of 107 ± 1.7, 72 ± 2.5, 80 ± 1.1, and 17 ± 1.3° corresponding to after a week of exposure to ambient air, O₂, CF₄, and Ar, respectively. It can be strongly reinforced that the stoichiometry and the adsorbates both play an important role in forming the hydrophobic TiO₂ films.

KEYWORDS: *flat TiO₂ film, anatase, natural hydrophobicity, fully stoichiometric TiO₂, hydrocarbon adsorbates, reversible wettability conversion*
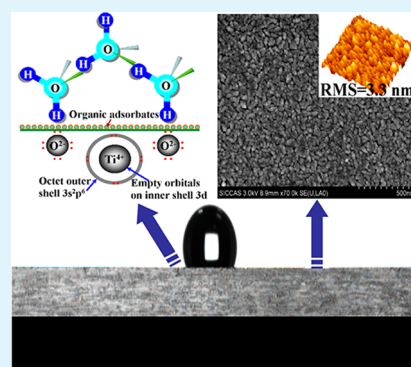
1. INTRODUCTION

Wettability is a very important property governed by both the chemical composition and the structure of solid surfaces.[1,2] The research of surface wettability over the past decades has attracted great interest because of its wide variety of applications.[3−5] Because of photoinduced super-hydrophilicity (contact angle (CA) of 0°), the crystal TiO₂ has already been applied as a transparent film with antifogging and self-cleaning properties.[6] In most cases, the TiO₂ films commonly tend to be hydrophilic (CA < 90°); however, the hydrophobic TiO₂ is also found on the rough surface (roughness over tens of nanometer) reported by some researchers.[7,8] With the development of the model from Wenzel (WM)[9] to Cassie and Baxter (C-BM)[10] during the last century, the relationship between wetting and surface roughness has been widely utilized for preparing and analysing the hydrophobicity.[11−14] Unfortunately, there is little work focused on the natural hydrophobicity of TiO₂ films with neglect of roughness. Actually, as antifogging and self-cleaning glasses, flat TiO₂ film (roughness <5 nm) can be more preferable because of high transmittance.

Recently, some researchers have reported a one-to-one correspondence between surface polarity, water-molecule orientation and wettability.[15] For common TiO₂ films, their surfaces can have a large number of polar sites because of oxygen-deficient and low-coordinated Ti atoms.[16] Nevertheless, a significant body of theoretical calculation has been devoted to understanding the interfacial water molecules in contact with the (101) anatase TiO₂ surface.[17] It can be conjectured that the hydrophobicity of flat TiO₂ film would be related with the orientation of interfacial water molecules. However, the origin of the hydrophobicity of the flat TiO₂ film is still not clear. In the present paper, we prepare the natural hydrophobicity of flat anatase TiO₂ thin films by DC reactive magnetron sputtering (DCRMS) at room temperature. Importantly, we attribute the cooperation effect of the stoichiometry of TiO₂ and the content of spontaneous adsorption of hydrocarbons onto the surface to determine the wettability of the flat TiO₂ films. In addition, we confirm the relationship between the surface compositions and the orientation of interfacial water molecules. Furthermore, the film surface shows the transition from hydrophobicity to super-hydrophilicity by alternation of UV irradiation and dark storage in ambient air.

2. EXPERIMENTAL SECTION

The flat TiO₂ films with 120 nm were deposited on n-type Si (100) wafers and plane glass slides by DC reactive magnetron
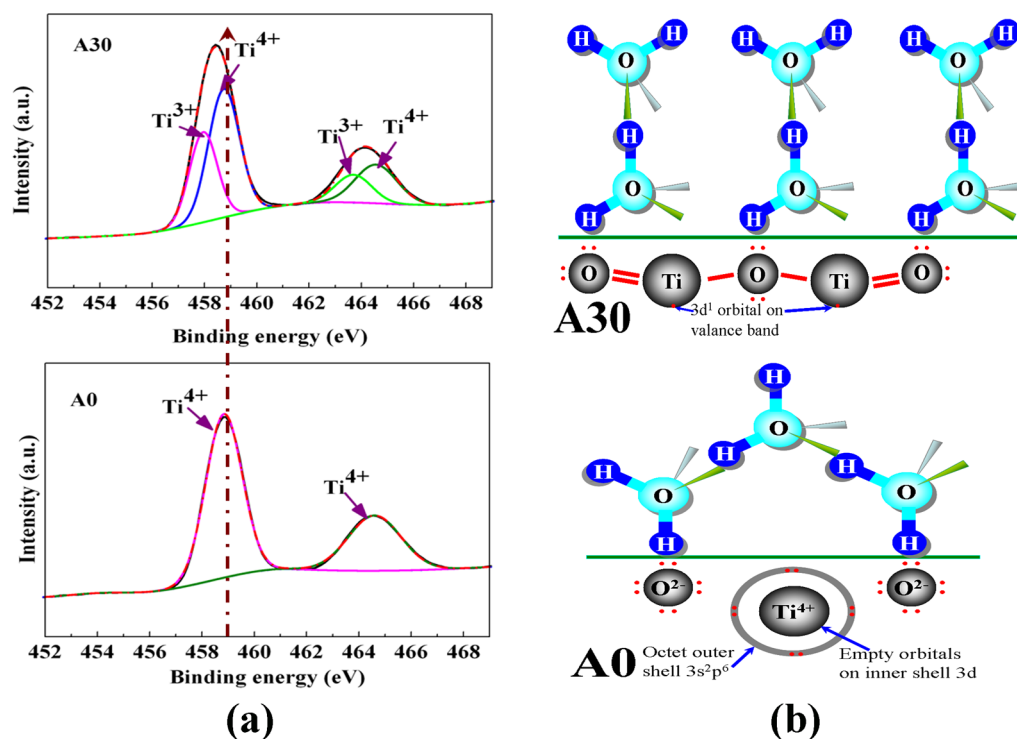
Figure 1. (a) XPS spectra of Ti 2p of film surface for the samples A0 (bottom) and A30 (top), respectively. (b) Schematic of the orientation of water molecules next to the surface of the samples A0 (bottom) and A30 (top), respectively (using different scales for the surface and water molecules).

sputtering with a Ti target (99.99% purity) at room temperature; further details are described in the Supporting Information. After film deposition, the part of as-prepared films were annealed in vacuum annealing furnace under 400 °C for 30 min. Thus, in this article, the films with 0 and 30 min of annealing time are presented as A0 and A30, respectively.

3. RESULTS AND DISCUSSION

To analyze the natural hydrophobicity of flat TiO_2 films, the chemical composition of the film surface was determined by XPS. Figure 1a is typical XPS spectra of film surface of the samples A0 and A30, both showing two major peaks for Ti 2p. It is found that the Ti $2p_{3/2}$ peak of the sample A30 is broader (full width at half-maximum (FWHM) ≈ 1.52 eV) at lower binding energy (458.4 eV) than that of the sample A0 (FWHM ≈ 1.47 eV, 458.8 eV binding energy). As proposed by Wang et al.,[18] the broadening of Ti $2p_{3/2}$ peak at low binding energy could be attributed to the presence of Ti^{3+} as well as the creation of oxygen vacancy on the surface of the sample A30. After performing the deconvolution with Lorentzian-Gaussian distribution function, the Ti $2p_{3/2}$ spectrum of the sample A30 displays two peaks at 458.8 and 457.9 eV, which are assigned to Ti^{4+} and Ti^{3+}.[19,20] Nevertheless, the sample A0 only has a 458.8 eV peak in Ti $2p_{3/2}$ spectrum corresponding to Ti^{4+} in TiO_2. It can be indicated that the surface of the sample A0 is nearly fully oxidized or free oxygen vacancy. It is known that the electronic charges of unfilled 3d orbital of Ti atoms are transfer to O atoms in TiO_2 surface, resulting in the full octet of electrons of $3s^2p^6$ orbitals in the outer shell.[17] Consequently, Ti atoms would have a lower tendency to exchange electrons and form a hydrogen bond with interfacial water molecules. Hence, the interfacial water molecules destroy their hydrogen-bonding network, and one OH bond from water molecules would be expected to joint with the surface oxygen atom through

hydrogen bonding while the remaining OH bond away from the surface, as shown in Figure 1b (down). The orientation of the interfacial water molecules mentioned above is usually an hydrophobic hydration structure,[21] which is in favor of the flat TiO_2 film to exhibit hydrophobic properties. In contrast, the electronic structure of Ti_2O_3 as like that of Al_2O_3[22] has a large number of polar sites originating from unsaturated atoms.[23] The Ti atoms at the surface are electron-deficient with seven electrons in their outer orbital. Thus, to obtain a stable state, Ti atom in Ti_2O_3 is prone to building a hydrogen bond with interfacial water molecule, leading to a hydrophilic hydration structure,[21] as sketched schematically in Figure 1b (up). Indeed, we observe water droplets to spread out on the surface of annealed TiO_2 film including a certain amount of Ti_2O_3, as shown in Figure 2d. This highlights the importance of chemical composition as well as electronic structure in the wettability of TiO_2 films.

Another reason for the hydrophobic state of the flat TiO_2 films can be related to the adsorption of organic molecules. Chemical and physical adsorption activity on the surface of various high energy materials is often driven by the tendency to reduce the total Gibbs free energy of the system by diminishing the surface energy part.[24−26] To confirm the adsorption of organic contaminants from the environment on the surface, infrared (IR) absorption spectra were measured at a grazing angle of 80°. As shown in Figure 2a, the characteristic alkyl C−H bond stretching vibrations of CH_2 and CH_3 groups were ubiquitous detected from our samples in the range 3000−2800 $cm^{−1}$.[24] This is direct evidence of the presence of the hydrocarbon contaminants. In addition, according to the absorption intensity of the spectra, it is easily indicated that the surface of the sample A0 adsorbed more hydrocarbon contaminants than that of the sample A30. To the best of our knowledge, TiO_2 films annealed at 400 °C can lead to
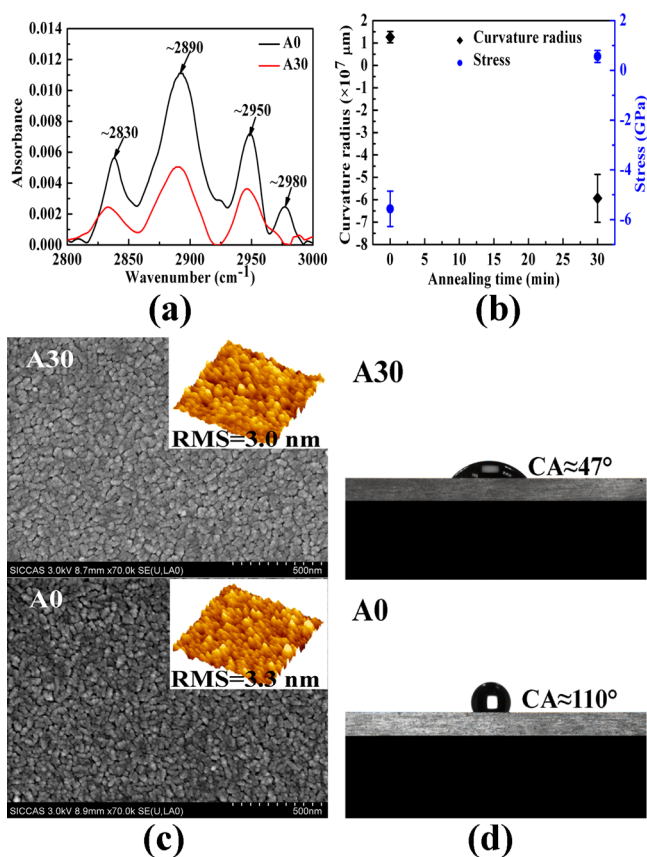
Figure 2. (a) IR absorbance spectra of the samples A0 and A30, respectively. (b) Curvature radius and the internal stress of the samples as a function of annealing time. (c) FESEM images of film surface of the samples A0 (bottom) and A30 (top), respectively (the insets are corresponding $2 \times 2 \ \mu m^2$ AFM images). (d) Water droplet shapes on the samples A0 (bottom) and A30 (top), respectively.

deposition rate and low deposition temperature. In addition, Figure 2c shows the surface morphology and microstructure of the samples obtained by atomic force microscopy (AFM) and field emission scanning electron microscope (FESEM). The root mean square (RMS) roughness of the samples A0 and A30 is 3.3 and 3.0 nm, respectively, making known the flat surface for both the samples. Such a small difference of the surface morphology between both the samples can hardly generate enormous difference in their CAs, according to the WM and C-BM theory.[9,10,27] However, as presented in Figure 2c, the surface of the sample A0 displayed more highly nonequilibrium nano grain boundaries than that of the sample A30. These nonequilibrium nano grain boundaries can enhance the adsorption capacity of the film surface. Besides, the surface of the sample A0 was (101) planes of anatase TiO_2, whereas the surface of sample A30 can include some (004) and (112) planes except (101) planes, determined by high resolution transmission electron microscopy (HRTEM) (shown in the Supporting Information). For anatase TiO_2, the sequence of the surface free energy of the crystal faces is (112) ≈ (001) > (101).[16,28] It should be pointed out that the relaxed (101) face of anatase TiO_2 still has very high surface energy (0.44 J m^{-2}), which is considered as hydrophilic material.[16] Thus, in this paper, we exclude the factors of surface roughness and crystalline orientation to probe the hydrophobic TiO_2 film. Furthermore, in basis of the contact angle tests, the samples A0 is a hydrophobic material and the water CA at flat surface is about 110 ± 1.5°, while the sample A30 with 47 ± 2.4° of CA is hydrophilic, as shown in Figure 2d. It is worth pointing out that the annealed film is difficult to recover the hydrophobicity even if leaves in the dark over two months. As mentioned above, the hydrophobicity of flat TiO_2 film can be ascribed to the fully or extremely approximately stoichiometric TiO_2 and hydrocarbon adsorbates on the film surface.

The spectra of water molecules near the surface of both the samples by using FTIR/ATR spectroscopy were applied to validate the orientation of interfacial water molecules, as given in Figure 3. It is necessary to point out that the FTIR/ATR with 45° of incidence angle can analyse an around 300 nm of water film. The broad band of vibrational spectrum of water between 3000 and 3800 cm^{-1} (the OH stretching region), which was yielded against the background spectrum of the clean diamond with the air, is deconvoluted into three peaks centred at around 3600, 3400, and 3200 cm^{-1}. The peaks at

relaxation of internal stress and grain boundaries to some extent, resulting in a decrease in total Gibbs free energy. The internal stresses of the samples measured by using the substrate bending method (shown in the Supporting Information) are shown in Figure 2b. Obviously, the stress value (0.56 GPa) of the sample A30 was positive, and lower than the absolute value of the stress (−5.57 GPa) of the sample A0. In fact, high compression stress in the sample A0 is produced by high
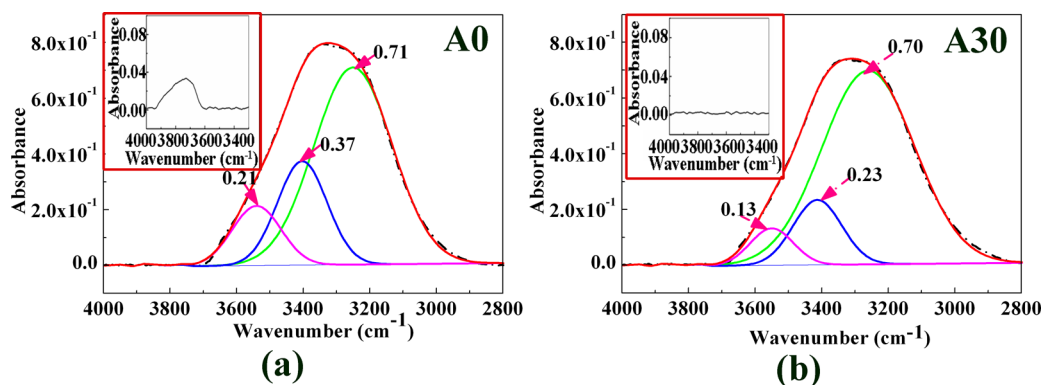

Figure 3. Original (black dashed curves) and deconvoluted (chromatic solid curves) spectra of interfacial water at the surface of the samples A0 (left) and A30 (right) against the background spectrum of the clean diamond with the air, respectively. (The insets are corresponding spectra of interfacial water against the background spectrum of the clean diamond with the water). The green, blue, and pink lines stand for the peaks centered at around 3600, 3400, and 3200 cm^{-1}, respectively.

3200, 3400, and 3600 cm^{-1} are ascribed to the OH stretching modes associated with the tetrahedral structure of bulk water molecules, to the hydrogen-bonded OHs straddling the interface and to non-hydrogen-bonded OHs pointing towards the surface, respectively.[23,29,30] Thus, it have been reported by other researchers that the peak at 3600 cm^{-1} had a higher magnitude at the surface of hydrophobic materials than that of hydrophilic materials.[23,29,30] As shown in Figure 3, the intensity of the peak at 3200 cm^{-1} is almost similar for both samples since it is attributed to the bulk OH stretching modes. However, the peak at 3600 cm^{-1} is higher for the sample A0 than that for the sample A30 by a factor of ~1.5. Furthermore, the peak at 3400 cm^{-1} also has a higher intensity for the sample A0 compared with that of the sample A30, indicating that the former surfaces have a higher number of OHs straddling the interface (as depicted in Figure 1b). To further distinguish the vibrational spectra of water at the surface of both the samples, the insets in Figure 3 shows the absorbance spectra of water against the background spectrum of the clean diamond with the water. It is interesting to note that the absorbance spectrum of water for the sample A0 has a peak at ~3700 cm^{-1}, whereas no peak is found in the sample A30. In fact, the peak at 3700 cm^{-1} can also be attributed to the non-hydrogen-bonded OHs pointing towards the surface.[30] Because the peak heights indicate the extent of hydrogen bonding in the interfacial water near the surface, these findings support that the orientation of water molecules near the surface of the as-prepared TiO$_2$ films is hydrophobic hydration structure.[23]

As a photosensitive material, the photoinduced hydrophilicity of the TiO$_2$ films was also worth to study and evaluate by water angle measurements. The water droplet shape on the flat surface of sample A0 is shown in Figure 4a (left), indicating the hydrophobicity (CA of 110 ± 1.5°). When the sample are

exposed to UV-light by Xe lamp (power 300 W, wavelength range from 250 to 400 nm) for 30 min, the water droplet spreads out on the surface and yields a CA of ~0°, as shown in Figure 4a (right). It is interestingly that after keeping in the dark with ambient air for 1 week, the wettability of the sample returns to hydrophobic again and the cycles can be repeated (Figure 4b). To further demonstrate the origin of the hydrophobic TiO$_2$ film and explore the mechanism of photoinduced hydrophilicity, we subjected the as-prepared TiO$_2$ films to the different atmospheres (air, Ar, O$_2$, and CF$_4$) after UV irradiation, as shown in Figure 4c. If not mentioned otherwise, the films were stored in dark environment. Apparently, contact angles for the film exposed to ambient air only increased slowly from ~0 to ~110° within 1 week after UV irradiation, which means the wettability of the film is reversible in the air. However, when the film was kept in pure Ar atmosphere, the surface still had strong hydrophilicity with CA of 17 ± 1.3°. The slight and gradual increase of CAs can be ascribed to the measurements of the contact angles carried out in room ambient. In addition, it is found in Figure 4c that the irradiated film in pure O$_2$ (CF$_4$) atmosphere quickly implemented the process of hydrophobization with CAs from ~0° to 72 ± 2.5° (80 ± 1.1°) within 2 days (1 day) and remained stable thereafter. These results can give some important information and conclusions. Interestingly, either fully stoichiometric TiO$_2$ of film surface or adsorbates with low surface energy on the surface hardly recovers the hydrophobicity of flat TiO$_2$ film with CA > 90°. In other words, only the combined action of both factors can yield a hydrophobic TiO$_2$ film. In addition, the film surface irradiated by UV light can simultaneously generate oxygen vacancies and remove the hydrocarbon adsorbates, which results in the photoinduced super-hydrophilicity of the TiO$_2$ film. Subsequently, when the film is exposed to the ambient air, the surface transforms into an energetically metastable state and reabsorbs the atmospheric oxygen[31] and organic contaminants, leading to the hydrophobicity on the surface again. Thus, the flat TiO$_2$ film shows the reversible conversion of superhydrophilic to hydrophobic by switching between UV-irradiation and dark storage.

4. CONCLUSION

In summary, flat TiO$_2$ thin films with natural hydrophobicity have been prepared by DC reactive magnetron sputtering at room temperature. The hydrophobicity of flat TiO$_2$ films is ascribable to the cooperation of fully or extremely approximately stoichiometric TiO$_2$ and hydrocarbon adsorbates on the film surface. Furthermore, we demonstrate that interfacial water molecules near the surface of the as-prepared TiO$_2$ film are oriented in the hydrophobic hydration structure via FTIR/ATR. In addition, the surface smart wettability for the as-prepared TiO$_2$ film is also realized by alternating UV-irradiation and dark storage.

■ ASSOCIATED CONTENT

Ⓢ Supporting Information

Detailed sample preparation, characterization, test methods, and structure of the samples. This material is available free of charge via the Internet at http://pubs.acs.org/.

■ AUTHOR INFORMATION

Corresponding Author
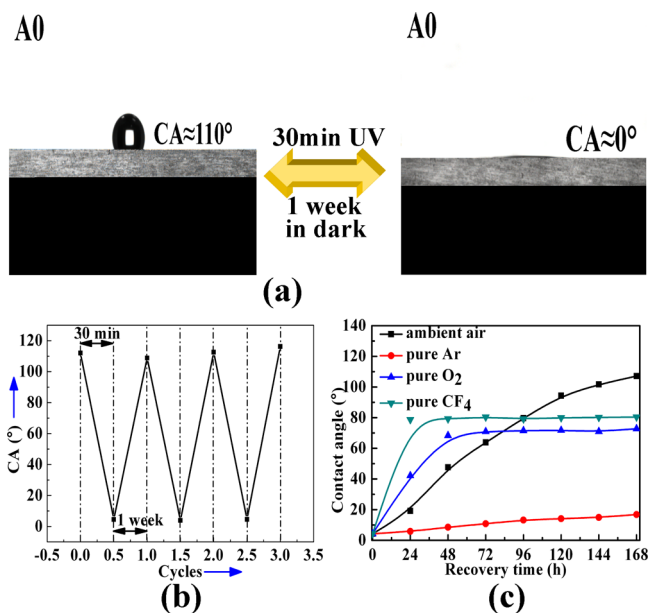*E-mail: p-jin@mail.sic.ac.cn.

Figure 4. (a) Photographs of a spherical water droplet with a CA of 110° (left) and a flat water film with a CA of 0° (right) before and after the sample A0 were exposed to UV illumination, respectively. (b) Reversible hydrophobicity/super-hydrophilicity transition of the sample A0 by alternating UV irradiation and storage in the dark. (c) Time-dependent evolution of contact angle for the sample A0 exposed to ambient air (■), pure Ar (●), pure O$_2$ (▲), and pure CF$_4$ (▼).

REFERENCES

(1) Feng, X. J.; Feng, L.; Jin, M. H.; Zhai, J.; Jiang, L.; Zhu, D. B. *J. Am. Chem. Soc.* **2004**, *126*, 62−63.

(2) Feng, L.; Li, S.; Li, Y.; Li, H.; Zhang, L.; Zhai, J.; Song, Y.; Liu, B.; Jiang, L.; Zhu, D. *Adv. Mater.* **2002**, *14*, 1857−1860.

(3) Parker, A. R.; Lawrence, C. R. *Nature* **2001**, *414*, 33−34.

(4) Wang, R.; Hashimoto, K.; Fujishima, A.; Chikuni, M.; Kojima, E.; Kitamura, A.; Shimohigoshi, M.; Watanabe, T. *Nature* **1997**, *388*, 431−432.

(5) Erbil, H. Y.; Demirel, A. L.; Avci, Y.; Mert, O. *Science* **2003**, *299*, 1377−1380.

(6) Carp, O.; Huisman, C. L.; Reller, A. *Prog. Solid-State Chem.* **2004**, *32*, 33−177.

(7) Sun, W. T.; Zhou, S. Y.; Chen, P.; Peng, L. M. *Chem. Commun.* **2008**, *44*, 603−605.

(8) Zhang, X. T.; Jin, M.; Liu, Z. Y.; Tryk, D. A.; Nishimoto, S.; Murakami, T.; Fujishima, A. *J. Phys. Chem. C* **2007**, *111*, 14521−14529.

(9) Wenzel, R. N. *Ind. Eng. Chem.* **1936**, *28*, 988−994.

(10) Cassie, A. B. D.; Baxter, S. *Trans. Faraday Soc.* **1944**, *40*, 546−550.

(11) Sun, T. L.; Wang, G. J.; Feng, L.; Liu, B. Q.; Ma, Y. M.; Jiang, L.; Zhu, D. B. *Angew. Chem., Int. Ed.* **2004**, *43*, 357−360.

(12) Leung, K. C. F.; Xuan, S. H.; Lo, C. M. *ACS Appl. Mater. Interfaces* **2009**, *1*, 2005−2012.

(13) Seo, J.; Lee, S.; Lee, J.; Lee, T. *ACS Appl. Mater. Interfaces* **2011**, *3*, 4722−4729.

(14) Liu, Y.; Lin, Z.; Lin, W.; Moon, K. S.; Wong, C. P. *ACS Appl. Mater. Interfaces* **2012**, *4*, 3959−3964.

(15) Giovambattista, N.; Debenedetti, P. G.; Rossky, P. J. *J. Phys. Chem. B* **2007**, *111*, 9581−9587.

(16) Lazzeri, M.; Vittadini, A.; Selloni, A. *Phys. Rev. B* **2001**, *63*, 155409−155417.

(17) Mattioli, G.; Filippone, F.; Caminiti, R.; Bonapasta, A. A. *J. Phys. Chem. C* **2008**, *112*, 13579−13586.

(18) Wang, L. Q.; Ferris, K. F.; Skiba, P. X.; Shultz, A. N.; Baer, D. R.; Engelhard, M. H. *Surf. Sci.* **1999**, *440*, 60−68.

(19) Courcot, D.; Gengembre, L.; Guelton, M.; Barbaux, Y.; Grzybowska, B. *J. Chem. Soc., Faraday Trans.* **1994**, *90*, 895−898.

(20) Werfel, F.; Brummer, O. *Phys. Scr.* **1983**, *28*, 92−96.

(21) Stirnemann, G.; Rossky, P. J.; Hynes, J. T.; Laage, D. *Faraday Discuss.* **2010**, *146*, 263−281.

(22) Greenwood, N. N.; Earnshaw, A. In *Chemistry of the Elements*, 1st ed.; House, L., Hill, J., Eds.; Butterworth-Heinemann: Oxford, U.K., 1997; Vol. *21*, p 961.

(23) Azimi, G.; Dhiman, R.; Kwon, H. M.; Paxson, A. T.; Varanasi, K. K. *Nat. Mater.* **2013**, *12*, 315−320.

(24) Boinovich, L. B.; Emelyanenko, A. M.; Pashinin, A. S.; Lee, C. H.; Drelich, J.; Yap, Y. K. *Langmuir* **2012**, *28*, 1206−1216.

(25) Toth, M.; Lobo, C. J.; Lysaght, M. J.; Vladár, A. E.; Postek, M. T. *J. Appl. Phys.* **2009**, *106*, 034306−034310.

(26) Xu, X.; Ren, B.; Wu, D. Y.; Xian, H.; Lu, X.; Shi, P.; Tian, Z. Q. *Surf. Interface Anal.* **1999**, *28*, 111−114.

(27) Chang, F. M.; Cheng, S. L.; Hong, S. J.; Sheng, Y. J.; Tsao, H. K. *Appl. Phys. Lett.* **2010**, *96*, 114101−114103.

(28) Wang, C.; Zhang, X.; Zhang, Y.; Jia, Y.; Yuan, B.; Yang, J.; Sun, P.; Liu, Y. *Nanoscale* **2012**, *4*, 5023−5030.

(29) Du, Q.; Freysz, E.; Shen, Y. R. *Science* **1994**, *264*, 826−828.

(30) Scatena, L. F.; Brown, M. G.; Richmond, G. L. *Science* **2001**, *292*, 908−912.

(31) Wang, R.; Sakai, N.; Fujishima, A.; Watanabe, T.; Hashimoto, K. *J. Phys. Chem. B* **1999**, *103*, 2188−2194.